Supplementary Information for

Bridging-droplet transfer from solid to porous surfaces

Kevin Murphy[1] and Jonathan Boreyko[2,*]

[1]Department of Biomedical Engineering and Mechanics, Virginia Tech

[2]Department of Mechanical Engineering, Virginia Tech

*boreyko@vt.edu

Image Processing:

The code was written from scratch for a local system in Java. The high speed videos were converted from Cine files to AVIs and then split to individual images for each frame. The images were ordered in folders given their frame count as a name. The pseudo code for the image analysis follows.

Inputs:

- Video name(Directs to folder)
- Frame rate
- Surface positions(in pixels)
- Beginning and end of analysis(frame numbers)
- Zoom factor used for the video
- Volume of the droplet
- Pore size
- Image averaging radius
- Wetting to wicking transition
- SHPB switch

1. For (All images)
    a. Create new image object
    b. For (All x)
        i. For (All y)
            1. Get average value for each pixel using averaging radius
    c. For (y between surface positions)
        i. Find max increase in pixel values(Right edge of bridge)
        ii. Find max decrease in pixel values(Left edge of bridge)
        iii. Save positions
    d. For (y between surface positions)
        i. Check if values are too different from nearby values
            1. Anything > (threshold) x coordinates away is marked
                a. 30 typical value used.
    e. Remove outlier points

f. Generate image showing raw data points taken to compare to raw image
g. Generate text file with the raw data points organized by y-position.
h. (Taylor series approximations were used to fill in gaps but this was determined to produce less accurate bridge captures and was not used in final processing)
i. Fit a polynomial to each of the bridge sides
    i. Attempted polynomial orders between order 2 and 5, order 4 was typically the most accurate.
        1. R^2 > 0.99 for most fits with coefficients having less than 1% error compared to fits generated in Excel.
j. Store polynomial coefficients
k. Generate text file with points used for fitting and the resulting coefficients

2. For (All images)
    a. Generate image plotting the two fits for the bridge shape between the two surfaces for comparison to raw data
3. For (All images)
    a. Calculate the desired information using the polynomial fits to get instantaneous/local values for first and second derivatives.
        i. Laplace pressures
        ii. Contact radii
        iii. Contact angles
    b. Store desired info in text files

An example of an experimental image and the two resulting images from the program are below.

Figure S1: The first image is a single frame directly from the video. The second image is the raw data points for the bridge shape and midline of the bridge. The third image is the fitted polynomials with the receiving contact diameter.

Calculated Viscous Wedge Height

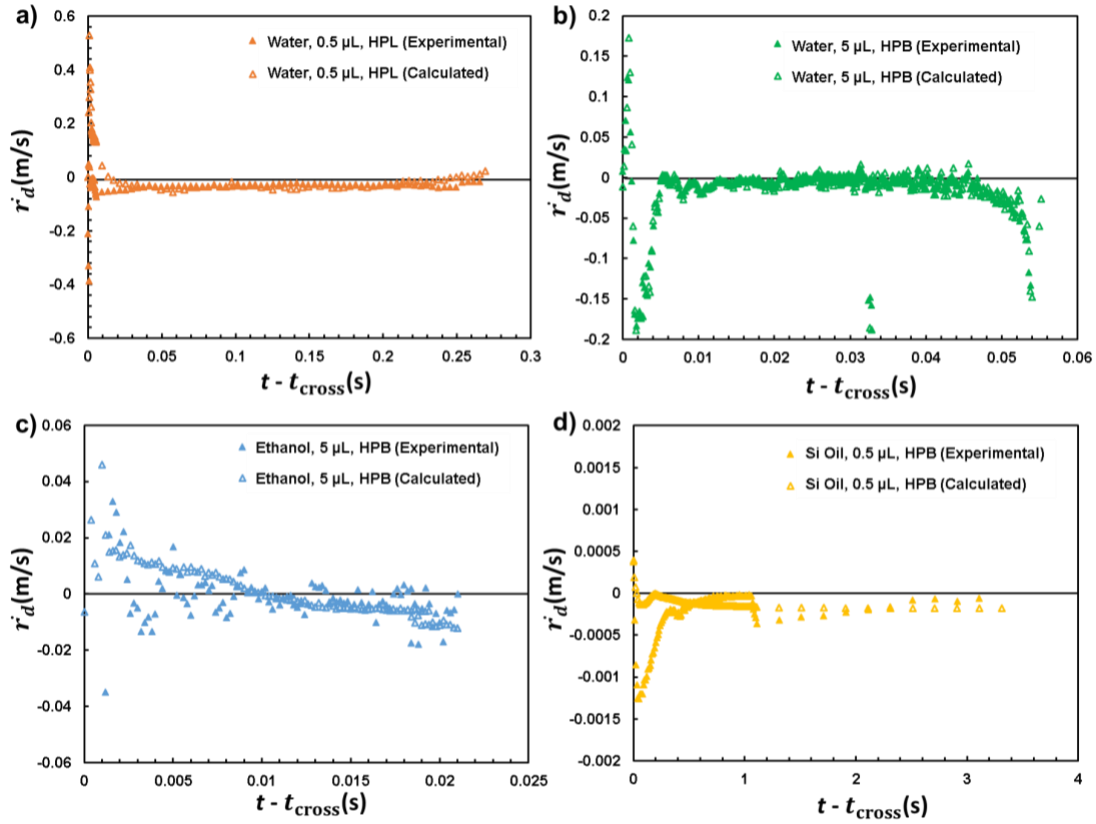

Figure S2: Experimental and theoretical donor contact line velocities in the donor-dependent wetting regime, using a fixed (i.e., averaged) h_μ value for each trial. Time is defined as $t - t_{cross}$, where t_{cross} is the duration of the preceding donor-independent wetting regime. Experimental data is shown by solid points while theoretical data is represented by empty points. Four cases are shown with different parameter sets: a) water, 0.5 µL, HPL, h_μ =11 µm, b) water, 5 µL, HPB, 1 µm, c) ethanol, 5 µL L, HPB, 20 µm, and d) Si oil, 0.5 µL L, HPB, 300 µm.

Four representative cases are graphed in figure S2 using an averaged value of h_μ for any given trial, rather than varying h_μ in time. The trends in the plots show a correlation between the Laplace pressure difference across the bridge, exemplified from the theoretical data, and the velocity of the donor contact radius. For the low viscosity cases, there can be a small increase in the donor radius temporarily. This occurs particularly in trials with short and wide liquid bridges, where there is very little room for the shape of the bridge to change, temporarily forcing some liquid outward, as parts of the liquid bridge above it change curvature. The global Laplace pressure measurements reflect this change, allowing the model to predict this temporary advancing behavior. This estimate of the receding contact line does not directly relate to the advancing contact line due to the indeterminate nature of the shape of bridge, but recall that the donor contact line velocity and the receiving contact line velocity scale with each other by conservation of mass.

Movie Captions

Movie S1: Bridging-droplet transfer corresponding to Fig. 2. The videos capture both the wetting and wicking regimes. Donor wettability is varied. Small flakes can be seen falling from the porous surface which we suspect to be microscopic pieces of the ceramic dislodged by the wetting process.

Movie S2: Bridging-droplet transfer corresponding to Fig. 2. These videos focus on the wetting regime, using a higher frame rate which necessitates a lower exposure and therefore darker videos.

Movie S3: Bridging-droplet transfer corresponding to Fig. 3, for varying working fluid, volume, and pore radius. The videos capture both the wetting and wicking regimes.

Movie S4: Bridging-droplet transfer corresponding to Fig. 3. These videos focus on the wetting regime, using a higher frame rate which necessitates a lower exposure and therefore darker videos. We do not show the video corresponding to Fig. 3d, as varying the pore radius does not appreciably affect the wetting regime by itself.